J. Membrane Biol. 9, 341 – 360 (1972)

Electrotonic Spread of Current in Monolayer Cultures of Neonatal Rat Heart Cells

H. J. Jongsma and H. E. van Rijn

Department of Physiology, University of Amsterdam,
1e Constantijn Huygensstraat 20, Amsterdam, The Netherlands

Received 28 December 1971

Summary. The passive electrical properties of neonatal rat heart cells grown in monolayer cultures were determined. Hyperpolarizing current pulses were injected through one microelectrode via an active bridge circuit. Membrane voltage displacements caused by the injected current pulses were measured at various distances from the first with a second microelectrode. Using a modified least-squares method the experimental results were fitted to a Bessel function, which is the steady-state solution of the differential equation describing the relation between membrane voltage caused by current injection and interelectrode distance in a very large and very thin plane cell. Best fit was obtained with a space constant of 360 μm and an internal resistivity of 500 Ω cm. From these figures, specific membrane resistance was calculated to be 1,300 Ω cm^2, assuming all current to leave through the upper surface of the monolayer.

The time constant of the membrane was measured from the time course of the current-induced membrane voltage displacements. From its value of 1.7 msec a membrane capacity of 1.3 μF/cm^2 was calculated.

From these results and some literature data on nexus distribution (A. W. Spira, *J. Ultrastruct. Res.* **34**:409, 1971) specific nexus resistance was calculated to range between 0.25 and 1.25 Ω cm^2, depending on the amount of folding of the intercalated discs. The results suggest that spread of activation in monolayer cultures of heart cells by means of local circuit currents is very likely.

Although Sjöstrand and Anderson (1954) showed that the heart consists of distinct cells, the general opinion still is that the heart behaves like a syncytium. Several investigators (Weidmann, 1952; Trautwein, Kuffler & Edwards, 1956; Van der Kloot & Dane, 1964) showed that intercellular resistance in different parts of the heart is so low that impulse transmission by local circuit currents is possible. Woodbury and Crill (1961) analyzed the two-dimensional electrotonic spread of current in rat atrium. They showed that the impulse, carried by local circuit currents from cell to cell, travelled easier into the fiber direction than perpendicular to it. This implies that low-

resistance cell junctions are to be found preferentially in the end regions of the cells.

Barr, Dewey and Berger (1965) presented evidence that specialized regions (nexuses) in the intercellular membrane systems (intercalated discs) are responsible for this low electrical resistance. Weidmann (1966) showed the intercalated discs to be of high ionic permeability. The value he calculated for specific disc resistance (3 Ω cm^2) compares very well with that predicted by Woodbury and Crill (1961) on the basis of a potential field analysis of the gap between the membrane regions forming the intercalated disc. Heppner and Plonsey (1970) confirmed their results. Similar values were found by Tanaka and Sasaki (1966) and Spira (1971).

A number of investigators (Sperelakis, Hoshiko & Berne, 1960; Lehmkuhl & Sperelakis, 1965; Tille, 1966; for a review *see*: Sperelakis, 1969) on the other hand, obtained evidence that intercalated discs have a high electrical resistance. In their opinion, impulse conduction is brought about by some kind of junctional transmission which may be of an electrical or chemical nature. The determination of the degree of electrotonus in heart muscle preparations is complicated by the geometry of these preparations. It is difficult to represent them by an adequate model.

To obviate this difficulty we decided to measure electrotonic interaction between rat heart cells in monolayer cultures. These monolayers consist of irregularly shaped but roughly circular cells with a diameter of 30 to 50 µm and a thickness of 3 to 6 µm. The cells contract rhythmically and contain myofibrils organized in bundles. The membrane regions where the cells contact each other are specialized into intercalated discs as shown by immunofluorescent labelling (Jongsma & Hollander, 1971) and electron microscopy (Cedergren & Harary, 1964). They have a simple, and well-defined geometry and are reasonably comparable to cells of the intact heart with regard to their physiological and morphological properties (Harary & Farley, 1963; Lehmkuhl & Sperelakis, 1963; Wollenberger, 1964). In this paper, we present the experimental results obtained from this preparation together with the conclusions that may be drawn from it concerning the passive electrical properties, assuming the monolayer to be a thin sheet with a length constant which is large compared to its thickness.

Theory

Introduction

A monolayer in which all cells are interconnected may be assumed to be a thin sheet with a parallel upper and lower surface. In this case, the resistance

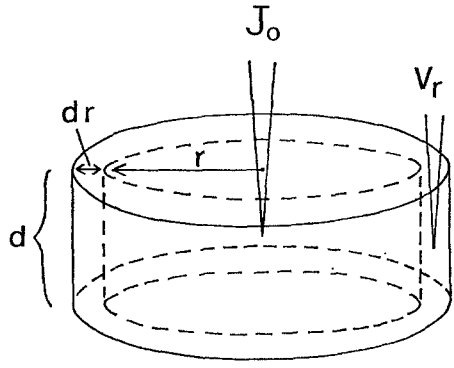

Fig. 1. Diagram illustrating parameters used to describe electrotonus in monolayers. Current is injected through electrode J_0; the resulting voltage displacement is measured with electrode V_r at distance r. d thickness of monolayer

of the intercellular connections is lumped together with the resistance of the cytoplasm. The area of the sheet is so large compared to its thickness that the sheet may be called infinite. When current is injected in the sheet at one place, it flows radially through the cytoplasm; part of it leaks out through the plasma membranes which form the upper and lower surfaces of the sheet. Therefore, the membrane potential displacement caused by the injected current decreases upon increasing the distance between the current-injecting electrode and the membrane potential recording electrode (*see* Fig. 1).

The steepness of the voltage decline depends, among other factors, on the surface area available for outward current leakage. In the present case, it is rather difficult to estimate to what extent the lower surface of the sheet (facing the bottom of the culture dish to which the cells are attached) contributes to the leakage area. In the mathematical description we included therefore a variable f ranging between 1 (no contribution of the lower surface) and 2 (entire lower surface contributes to leakage area), to account for this uncertainty.

Symbols Used

$V_{r,t}$ = membrane voltage at distance r and time t

$J_{r,t}$ = radial current at distance r and time t

J_0 = amount of current injected

j_m = membrane current density at distance r and time t

ρ_i = resistivity of cytoplasm + intercellular connections

R_m = resistance of 1 cm^2 of plasma membrane

C_m = membrane capacitance

$\tau = R_m C_m$ = membrane time constant

t = time after onset of current

$T = t/\tau$

r = distance between electrodes

d = thickness of monolayer

f = fraction of lower surface contributing to current leakage; $1 \leqq f \leqq 2$

$n = \rho_i / 2\pi d$

K_0 = zero order Bessel function of the second kind with imaginary argument (Abramowitz & Stegun, 1964)

$\lambda = \sqrt{R_m d / \rho_i f}$ = space constant.

Mathematical Description

The voltage drop over the cytoplasmatic and intercellular resistance in the radial direction is given by

$$\frac{\delta V_{r,t}}{\delta r} = -J_{r,t} \frac{\rho_i}{2\pi r d}. \tag{1}$$

The current drop in the radial direction caused by current leakage through the upper and lower surface of the monolayer is given by

$$\frac{\delta J_{r,t}}{\delta r} = -2\pi r f j_m = \frac{2\pi r f}{R_m} \left(V_{r,t} + \tau \frac{\delta V_{r,t}}{\delta t} \right). \tag{2}$$

Introducing the space constant λ and combining Eqs. (1) and (2) we obtain the differential equation

$$\frac{\delta^2 V_{r,t}}{\delta r^2} + \frac{1}{r} \frac{\delta V_{r,t}}{\delta r} - \frac{1}{\lambda^2} V_{r,t} = \frac{\tau}{\lambda^2} \frac{\delta V_{r,t}}{\delta t}. \tag{3}$$

The well-known solution of this equation is (*see* e.g. Shiba, 1971)

$$V_{r,t} = n J_0 \int_0^T \tfrac{1}{2} u \exp(-u - r^2/4\lambda^2)\, du. \tag{4}$$

In the steady state, this solution reduces to

$$V_{r,\infty} = n J_0 K_0(r/\lambda). \tag{5}$$

To obtain the passive electrical properties of the preparation using this model, the measured membrane voltage displacements divided by the applied current strength are plotted against the distance between the electrodes at which they are measured. Using a modified least-squares method the best-fitting Bessel function is found. In this way n and λ are found and from these the constants R_m and ρ_i can be calculated.

To estimate C_m the time course of the membrane voltage displacements at any distance, caused by the injected current pulse, is numerically differentiated. Using the least-squares method τ is then found by fitting the values obtained to the derivative of the time dependent solution [Eq. (4)] of the differential Eq. (3):

$$|\delta V_{r,t}/\delta t| = (n\,|J_0|/2t)\exp(-t/\tau - r^2\tau/4\lambda^2 t). \tag{6}$$

C_m is then calculated from the relation

$$\tau = R_m C_m. \tag{7}$$

Methods

Tissue Culture Technique

Monolayers of heart cells were prepared as described by Harary and Farley (1963). In brief, 12 hearts of two-day-old Wistar rats were excised as aseptically as possible. After removal of blood vessels, the hearts were cut in small pieces and incubated at 37 °C with 25 ml of a 0.1 % trypsin solution in Pucks saline A (Marcus, Cieciura & Puck, 1956). After a pre-incubation of 30 min the procedure was repeated three times for 20 min, each time with a fresh aliquot of trypsin solution. The resulting cell suspensions were centrifuged (3 min; $600 \times g$). The pellets were washed two times with 2 ml of complete growth medium (CGM). The final suspensions were pooled and counted with a haemocytometer. The cells were plated in plastic petri dishes (Falcon plastics, $\varnothing$ 51 mm) and CGM was added to obtain a final cell concentration of 5×10^5 cells/ml. The dishes were incubated at 37 °C in an atmosphere of air and CO_2 with a relative humidity of 80 to 90%. The pH in the culture dishes ranged between 7.2 and 7.3. The medium was changed every 48 hr.

After 5 to 7 days of culturing, the preparations were used for experimentation. The CGM was a modification of the growth medium of Puck (Marcus *et al.*, 1956) consisting of a Hanks balanced salt solution containing amino acids and vitamins, 10% human serum, 10% fetal calf serum and penicillin. Streptomycin was omitted from the original formulation, because in our hands it inhibited growth and rendered the heart cells insensitive to autonomous drugs. The ionic composition of the medium in mM included: 145.1 Na^+, 4.7 K^+, 1.4 Ca^{2+}, 0.7 Mg^{2+}, 138.6 Cl^-, 17.5 HCO_3^-, as checked with atomic absorption spectrophotometry.

Experimental Procedure

Cultures were placed on the stage of an inverted microscope (Reichert MeF″2, total magnification either 128 or 320×, depending on interelectrode distance) and kept at a constant temperature of 33 ± 0.1 °C. Evaporation was checked by layering

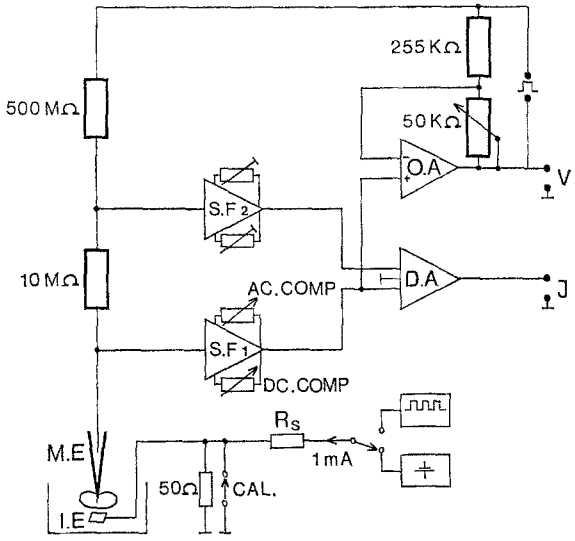

Fig. 2. Schematic diagram of the active bridge circuit. By applying the stimulus floating between the output of the operational amplifier (*OA*) and the bridge resistances, shunting of the input impedance of the source-follower (SF_1) was prevented. After balancing the bridge with the 50-kΩ resistor, the stimulus is virtually absent in the output signal. The bridge resistances are heavy-lined. SF_2 current measuring source-follower; *DA* differential amplifier

a little paraffin oil on top of the medium. Changes in pH during the experiments were small; pH measured before and after experimentation ranged always between 7.2 and 7.4.

In preliminary experiments, cultures kept beating with a constant rate for several days under the experimental conditions mentioned. Current pulses were injected through one microelectrode and changes in membrane voltage caused by these pulses were measured with a second microelectrode at varying distances from the first one. Conventional glass microelectrodes filled with 2.7 M KCl + 2 mM K-citrate ($R = 15$ to 40 MΩ) (Politoff, Socolar & Loewenstein, 1969) were used. Via chlorided silver wires both microelectrodes were connected to the input stage of a source follower with input capacity compensation (0 to 100 pF) and d−c offset adjustment. Gate current was 10^{-12} amps, d−c input impedance $>10^{12}$ Ω, input impedance at 1 KHz $>3 \times 10^9$ Ω and risetime <50 μsec through a 30 MΩ electrode with compensated capacity.

The system was calibrated by applying a 50-mV signal to the reference electrode. An agar-salt bridge was used as reference electrode. Therefore the d−c offset potential before impaling cells was mainly caused by the tip-potential of the microelectrode. In the experiments described, the d−c offset potential never exceeded 5 mV.

Both microelectrodes were mounted in an active bridge circuit (Fig. 2) which made it possible to apply current and measure membrane potential simultaneously without shunting the input impedance of the source follower with the bridge resistances, as is the case in the classical bridge circuit described by Frank and Fuortes (1956). As shown in Fig. 2, current was measured as the voltage drop across a 10 MΩ precision resistor with a second source follower.

Constant current pulses (2 to 20 namps hyper- and depolarizing current; duration 70 to 100 msec) were generated with a Grass S4 stimulator which was, via a stimulus

isolation unit, connected in series with the 500 MΩ resistor and the microelectrode. A delayed trigger circuit made it possible to apply pulses at any desired moment in the cardiac cycle. To eliminate small fluctuations of membrane potential, current pulses were applied during every other action potential.

The distance between the electrode tips was estimated with a calibrated eyepiece graticule. Current and voltage output from both bridges was amplified, monitored on a dual beam oscilloscope (Hewlett-Packard 132a) and stored on an Ampex FR 1300 instrumentation recorder for off-line data processing.

Data Processing

The action potentials recorded at various distances from the current-injecting electrode were digitized with an A−D converter (DIDAC 800; Intertechnique) and printed. The difference between the steady-state voltage during diastole and during the pulse was calculated by subtracting the action potential with pulse from the action potential without. This value was divided by the applied current; the resulting value in MΩ was plotted against the interelectrode distance and used for the curve-fitting procedure described in the Appendix.

Results

After 5 to 7 days of incubation, the initially isolated heart cells grew into a confluent monolayer in which all myoblasts beat synchronously. This synchrony is established already after two days in culture (Jongsma & Hollander, 1971) but at that time the monolayer is not yet confluent which makes impalement rather troublesome.

Action potentials recorded from these monolayers are shown in Fig. 3. Mean amplitude was 87.3 ± 7.3 mV ($n = 48$); in a few cases we measured

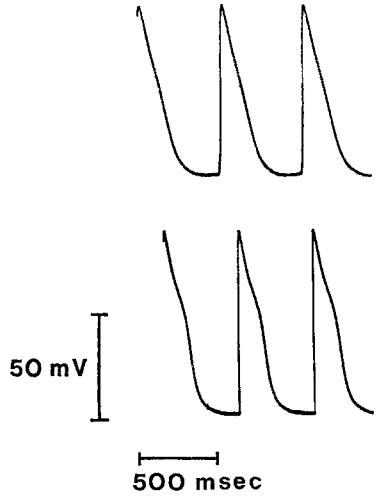

Fig. 3. Action potentials from cultured rat heart cells. *Upper trace:* action potentials from a 6-day-old monolayer; *Lower trace:* action potentials with a considerable plateau from a 7-day-old monolayer

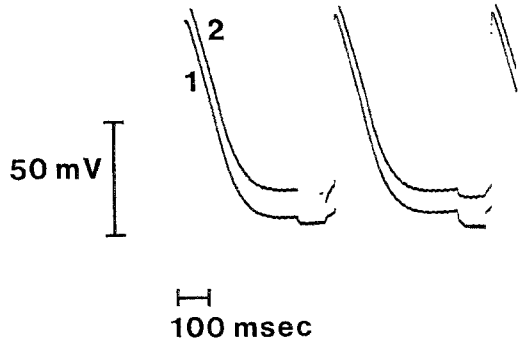

Fig. 4. Pairs of action potentials recorded at 74 μm interelectrode distance illustrating absence of intercellular rectification. In the first pair, hyperpolarizing current (11 namps; 100 msec) was passed through electrode 2, recording trace 2; only the end of the pulse is seen because of bridge unbalance. The resulting membrane potential displacement is shown in trace 1 recorded with electrode 1. In the second pair the situation was reversed; in this case a 13-namp, 100-msec hyperpolarizing current pulse was passed through electrode 1. $V_{r,\infty}/J_0$ in the first pair equals $V_{r,\infty}/J_0$ in the second pair

the overshoot which ranged between 18 and 21 mV. As shown in Fig. 3, some action potentials exhibited a plateau phase whereas in other cases repolarization proceeded smoothly.

Fig. 4 shows pairs of action potentials recorded at 74 μm interelectrode distance. Constant hyperpolarizing current pulses were passed first through one electrode and the resulting membrane potential displacement was measured with the other. The situation was then reversed. In all cases tested, there was no difference in the magnitude of the measured membrane potential displacement. It seems safe therefore to conclude that intercellular connections between cultured heart cells have no rectifying properties. In the range of current strengths used the monolayers behave electrically like linear networks as indicated in Fig. 5. The relation between current and voltage is a straight line. This suggests that the membrane properties measured are passive properties indeed, although it is possible that linearizing effects in the monolayer mask a certain amount of nonlinearity in membrane behavior (Noble, 1962). In any event, this observation justifies the normalization procedure we used to compare experiments in which current pulses of different strength were applied.

Fig. 6 gives an example of an electrotonic pulse obtained at an interelectrode distance of 82 μm after processing two consecutive action potentials as described under Methods.

This procedure was repeated at as many distances as possible in one culture and in 25 different cultures. Only those recordings in which both

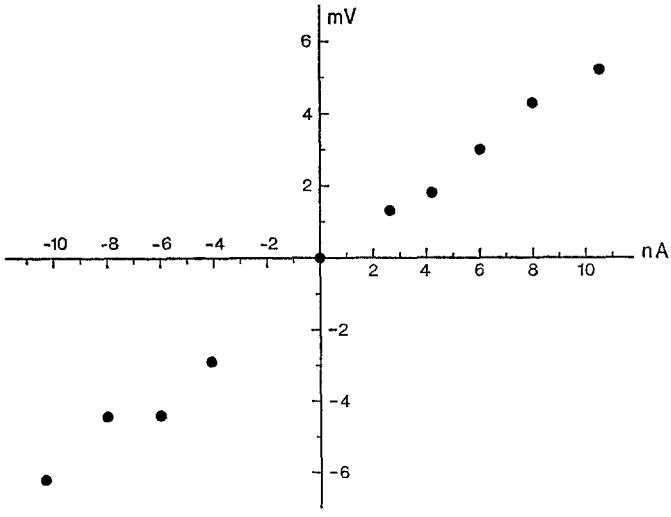

Fig. 5. Relationship between steady-state electrotonic potential and applied current strength at fixed interelectrode distance (100 μm)

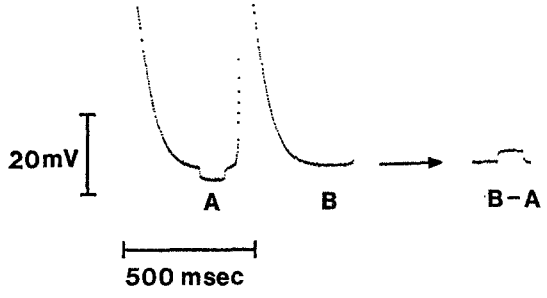

Fig. 6. Two consecutive action potentials from the voltage-recording electrode. 250 msec after the beginning of the first action potential a hyperpolarizing current pulse of 10 namps and 100-msec duration was applied at a distance of 82 μm. The first action potential was then subtracted from the second one during which no current pulse was delivered. The resulting signal is shown at right ($B-A$)

action potentials measured 80 mV or more were used. Care was taken to select for the curve-fitting procedure only those pulses where the membrane potential displacement reached a steady value within the pulse duration.

Fig. 7 shows the resulting relationship between membrane voltage displacement and interelectrode distance. Each point is the mean of the amplitude of five consecutive pulses. Also shown in Fig. 7 is the Bessel function that fits best to the experimental points. This best fit was obtained with $\lambda = 360$ μm and $n = 0.16$.

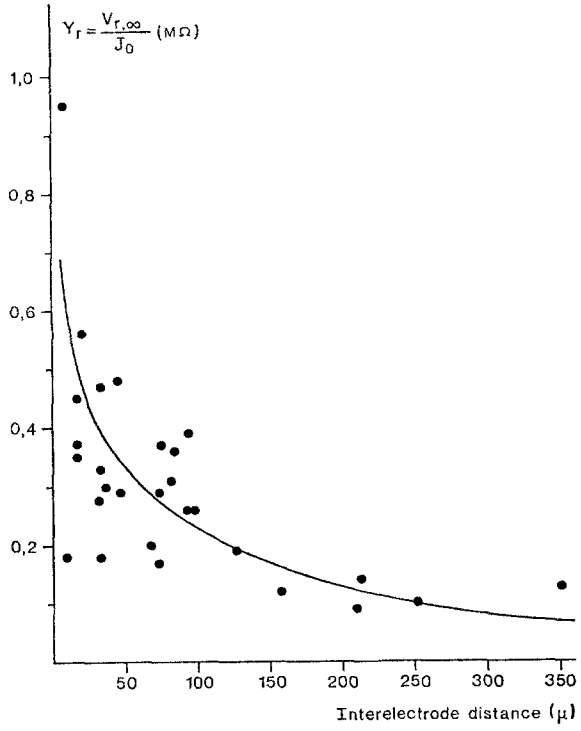

Fig. 7. Relationship between steady-state voltage displacement and interelectrode distance. Dots are those experimental results obtained from 25 cultures where both action potentials measured at least 80 mV and the membrane voltage displacement became steady within the pulse duration. Each dot is the mean of five consecutive amplitude measurements

To calculate the passive electrical properties from these values, the thickness of the monolayer must be known. From transverse sections of some preparations, we estimated this thickness to be about 5 μm.

To estimate disc resistance from our results we assume all discs to lie on rings (radius r) spaced one cell-length (p cm) apart; nexus density is a/cm; area of each nexus is O cm^2. Total area of nexus in each ring $2\pi r a O$; total area of each ring is $2\pi r d$ (d = thickness of sheet).

If $g = \frac{\text{total area nexus}}{\text{total area intercalated disc}}$ then

$$2\pi r a O = g 2\pi r d \rightarrow a O = g d. \tag{8}$$

When ρ_d is nexus-resistivity and Δ thickness of nexus, the nexal resistance is

$$\frac{\rho_d \Delta}{2\pi r a O} \Omega. \tag{9}$$

When it is assumed for simplicity that this resistance is distributed over one whole cell, then nexal resistance becomes

$$\frac{\rho'_d p}{2\pi r d}\Omega \tag{10}$$

where ρ'_d is the distributed resistivity of the nexus. Thus,

$$\frac{\rho_d \Delta}{2\pi r a O}=\frac{\rho'_d p}{2\pi r d}. \tag{11}$$

Now combining Eqs. (8) and (11) we have

$$\rho'_d=\frac{\rho_d \Delta}{p g}=\frac{R_d}{p g}\Omega\,\mathrm{cm}; \tag{12}$$

(R_d = specific nexus resistance)

$$\rho_i=\rho_c+\rho'_d. \tag{13}$$

Because we lumped the cytoplasmatic (ρ_c) and nexal (ρ'_d) resistivity together in our original formulation (*see* Theory) it follows now from Eqs. (12) and (13) that

$$\rho_i=\rho_c+\frac{R_d}{p g}. \tag{14}$$

Because of the fact that the intercalated disc between two cells is not a flat plane but rather intricately folded, a folding factor F has to be included; it is easily shown that Eq. (14) converts then to

$$\rho_i=\rho_c+\frac{R_d}{p g F}. \tag{15}$$

If we take $\rho_i=500\ \Omega\,\mathrm{cm}$ (this paper), $\rho_c=120\ \Omega\,\mathrm{cm}$ (Schanne, 1969), $p=30\ \mu\mathrm{m}$ (this paper), $g=0.11$ (Spira, 1971), $F=2$ to 10 (Woodbury and Crill, 1961; Spira, 1971), then $R_d=0.25$ to $1.25\ \Omega\,\mathrm{cm}^2$ depending on the amount of folding.

Table 1 contains the passive electrical properties we calculated from our results together with the values given by some other authors.

Table 1. Passive electrical properties of heart cells

Preparation	λ (μm)	R_m (Ω cm^2)	R_d (Ω cm^2)	ρ (Ω cm)	C_m (μF/cm^2)	Reference
Rat heart	362	1316	0.25–1.25[a]	502	1.3	This paper ($f=1$)
(tissue culture)	362	2632	0.25–1.25[a]	502	0.65	This paper ($f=2$)
Rat heart (tissue culture)	650	5516	—	542	—	Hyde *et al.* (1969)
Sheep ventricle (trabeculae)	960	9100	—	470	0.81	Weidmann (1970)
Sheep Purkinje fiber	1900	1940	—	154	12.4	Weidmann (1952)
Sheep Purkinje fiber[b]	1550	—	3.0	—	—	Weidmann (1966)
Dog atrium	1240	5593	—	261	1.0[c]	Sakamoto and Goto (1970)
Rat atrium	130	~500	<1.2	—	—	Woodbury and Crill (1961)
	170	~1000	~6	1500	—	Woodbury (1962)
Mouse ventricle	70–500	—	<2.0	—	—	Tanaka and Sasaki (1966)

[a] Depending on folding factor.
[b] Data from diffusion experiments with ^{42}K.
[c] Assumed value.

Discussion

The Model

To estimate the passive electrical properties of the described monolayer of heart cells, a model has to be chosen which represents it as accurately as possible. Several models are reported to describe a two-dimensional preparation. All of these lead to the same differential equation relating voltage displacement to interelectrode distance.

Most models are discrete; e.g., the honeycomb structure proposed by Siegenbeek van Heukelom (1971) for epithelial cells and the branching fiber models for myocardial preparations discussed by George (1961) and Tanaka and Sasaki (1966). Woodbury and Crill (1961) represented their rat atrial wall preparation by a continuous thin-plane cell model: a two-sided slab of cytoplasm bounded by parallel upper and lower surfaces of plasma membranes; the resistance of the intercellular membranes is lumped together with that of the cytoplasm.

The same model was used by Hyde, Blondel, Matter, Cheneval, Filloux and Girardier (1969) to represent their heart cell monolayers.

Both groups of authors, however, failed to take into account (at least in their mathematical description of the model) that current flows out through both surfaces as pointed out also by Eisenberg and Johnson (1970).

Woodbury (1962) obtained a value of 170 μm for λ. He ascribed this low value to the presence of a greater area of plasma membrane in the preparation than might be inferred from the model. Although his experimental points fit well to a Bessel function, it might be that the thick-plane cell model, as discussed by Eisenberg and Johnson (1970) would accommodate the data even better and furnish a larger space constant.

In our case, we have a monocellular layer of interconnected cells in which no fiber tracts are detectable in a large bath of extracellular fluid.

Heart cells in monolayer culture have an irregular shape. Intercalated discs are found around the entire cell perimeter; consequently, there should be no directional influence on the magnitude of the space constant as is the case in the rat atrial wall preparation used by Woodbury and Crill (1961). Indeed, we never found any influence of electrode orientation on electrotonus. Therefore, it seems that the thin-cell model is a fairly accurate description of our preparation.

As might be seen from Fig. 7, we did not detect discontinuities in the voltage-distance plot, which is an indication that the resistance of the intercellular membranes is so low that it may be lumped together with the resistance of the cytoplasm. The same view is adopted by Tanaka and Sasaki (1966) who only detected a discontinuity at very small interelectrode distances. They attributed this discontinuity to the voltage gradient that exists between the tip of the current electrode and the cell membrane very near this electrode.

Eisenberg and Johnson (1970) calculated the influence of electrode positioning on the relation between voltage displacement and interelectrode distance. They found a relation consisting of two parts. One part, depending on the passive membrane properties, is the same as our steady-state solution and the other part depends on the position of the electrodes in the sheet.

In the region of small interelectrode distances ($r < d$), the curve relating voltage to distance is steeper than the Bessel function, but at interelectrode distances greater than the thickness of the sheet, the contribution of the electrode positioning is negligible.

Because the smallest distance at which we measured (8 μm) is larger than the thickness of the monolayers we used (5 μm), there is no need to account in our calculations for this factor.

An objection may be made against the use of monolayers prepared from trypsinized hearts to determine the passive electrical properties of heart cell membranes: the monolayers contain not only heart cells but also fibroblasts. In tissue culture, these two kinds of cells grow together and interact electrically as shown by Hyde *et al.* (1969) and by Goshima (1970). In this way, the passive electrical properties measured are not those of heart cells *per se* but those of a mixture of cells.

To what extent in whole hearts connections between myocardial cells and connective tissue cells are present is unknown. From the results of Hyde *et al.* (1969) it seems that fibroblasts tend to lower the space constant, mainly by lowering the membrane resistance.

Lehmkuhl and Sperelakis (1965) failed to show substantial electrotonic interaction in monolayers of cultured heart cells. They attributed this to high disc resistances. The reported input resistance of 12.6 MΩ (Sperelakis & Lehmkuhl, 1964) supports this idea. As a model, however, they used a semi-infinite cable, although morphologically monolayers have no cablelike features.

For an infinite cable, the relation

$$V = n J_0 e^{-r/\lambda} \tag{16}$$

holds, whereas for a two-dimensional sheet

$$V = n J_0 K_0(r/\lambda). \tag{17}$$

The input resistance is defined as

$$Z_0 = V_0/J_0 \tag{18}$$

(V_0 is voltage displacement at $r=0$ due to injected current J_0).

Thus, for a cable

$$Z_0 = n \tag{19}$$

whereas for a sheet

$$Z_0 = n K_0 \quad (K_0(r/\lambda) \to \infty \quad \text{as} \quad r \to 0). \tag{20}$$

Thus, "Z_0" in a sheet is very high because at $r=0$ the mathematical description of the model has no physical meaning. Moreover, when we calculate the best-fitting exponential function to our data, using the least-squares method, the fit is considerably worse ($P=0.135$; *see* Appendix) than that of the Bessel function ($P=0.09$). Using the cable equation a space constant

of 156 μm is found. It therefore seems that both the high input resistance and the lack of substantial electrotonic interaction are caused by choosing a cable model instead of an thin-plane cell model to represent the monolayer.

The Passive Electrical Properties

As shown in Table 1, the passive electrical properties we calculated from our results are comparable to those found by Hyde *et al.* (1969) for their mixed cultures. These values were obtained from the Bessel function shown in Fig. 7. From this figure it can be seen that there is quite an amount of scatter in the experimental points. This may be caused by the fact that our experimental data were obtained from many different cultures. Also, it must be pointed out that the measurement of the interelectrode distance was not very accurate because of the difficulty in exactly locating the very tip of the microelectrodes.

The values we find for R_m and C_m compare reasonably well with those obtained by Weidmann (1970) for ventricular trabeculae and also with those of Sakamoto and Goto (1970) for dog myocardium.

The membrane capacitance is in accord with that found by others except for the value Weidmann (1952) gives for Purkinje fibers. Folding of the Purkinje fiber membrane may be the cause of this discrepancy.

The internal resistance we find is somewhat higher than that reported for heart cells generally; this is to be expected from the somewhat small size of our heart cells when it is assumed that the bulk of internal resistance is located at the intercalated discs, because there will be more intercalated discs in a given area of the preparation than in preparations with larger cells.

Weidmann (1966) found a disc resistance of about 3 $\Omega\,cm^2$ from his diffusion experiments with radioactive potassium. Such values are also reported by Tanaka and Sasaki (1966) for mouse myocardium and by Woodbury and Crill (1961) for rat atrium. Recently, Spira (1971) calculated a value of 1.4 $\Omega\,cm^2$ for dog myocardium based on morphological observations.

Almost all authors agree that these values are the highest possible estimates and that the actual disc resistance might be lower. In fact, Woodbury and Crill (1970) recently revised their estimated disc resistance down to 0.3 $\Omega\,cm^2$.

Using a line of reasoning somewhat analogous to Spira (1971) we calculated disc resistance in our preparations to range between 0.25 and 1.25 $\Omega\,cm^2$, depending on the amount of folding of the intercalated disc.

Although this estimation is admittedly an over-simplification, the value found for R_d compares closely with the cited literature values.

In epithelial tissues, junctional membrane resistance is of the same order of magnitude: Loewenstein, Socolar, Higashino, Kanno and Davidson (1965) found a junctional resistance of 0.6 to 1 $\Omega\,cm^2$ in *Chironimus* salivary gland. In *Drosophila* salivary gland, junctional resistance ranges between 0.3 and 12 $\Omega\,cm^2$ (Loewenstein & Kanno, 1964). Siegenbeek van Heukelom (1971) reported a junctional membrane resistance of 10 to 100 $\Omega\,cm^2$ for monolayers of cultured epithelial cells of embryonal chick intestine. In these tissues, flow of dyes and ions from one cell to the next was demonstrated (*see* e.g., Azarnia & Loewenstein, 1971).

The fact that specific nexus resistance is about 1,000 times lower than plasma membrane resistance, makes spread of activation by local circuit current, presumably carried by potassium ions (Weidmann, 1966), very likely.

Appendix

In the Results section we found a set of points $G(y_r, r)$ where

$$y_r = \frac{V_{r,\infty}}{J_0} \tag{A.1}$$

the measured voltage displacement divided by the applied current. In the theoretical case

$$y_r = nK_0(r/\lambda). \tag{5}$$

Because the normal least-squares method does not render explicit functions for n and λ we used a modified method.

Let S be the sum of the squared deviations from the theoretical curve, i.e.

$$S = \sum_G (y_r - nK_0(r/\lambda))^2. \tag{A.2}[1]$$

The best-fitting n and λ are found when S is minimal, which is the case for

$$(\delta S/\delta n)_\lambda = 0 \tag{A.3}$$

or

$$(\delta S/\delta \lambda)_n = 0. \tag{A.4}$$

1 To compare different sets of points, an entity P can be defined as follows

$$P = \frac{S}{\sum_G y_r^2}. \tag{A.2.1}$$

P ranges between 0 and 1 and is independent of the number of experimental points (y_r, r) used.

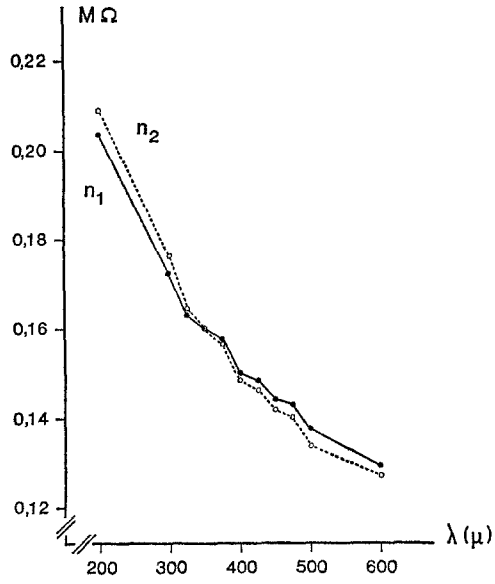

Fig. 8. Relationship between n_1, n_2 and λ; curves intersect at the best n and λ

From (A.3) and (A.4) we get two explicit expressions for n:

$$n_1 = \frac{\sum_G y_r K_0(r/\lambda_1)}{\sum_G K_0^2(r/\lambda_1)}, \tag{A.5}$$

$$n_2 = \frac{\sum_G r\, y_r K_1(r/\lambda_2)}{\sum_G r K_0(r/\lambda_2) K_1(r/\lambda_2)}. \tag{A.6}$$

n_1 and n_2 are both monotonously descending functions of λ, so there is only one point of intersection. We can find the best n and λ by choosing a series of λ's and calculating the values of n_1 and n_2 from (A.5) and (A.6). After plotting these against λ, the point of intersection is located (*see* Fig. 8).

In the neighborhood of the intersection point, $(n_1 - n_2)$ is extremely small.

To get a better approximation, $(n_2 - n_1)$ is calculated and plotted at a larger scale against λ. At the best λ this curve intersects with the λ-axis (Fig. 9). The best n is then found from the original n_1 against λ plot. Once n and λ are found, R_m and ρ_i are calculated from the relations

$$\rho_i = 2\pi n d \tag{A.7}$$

$$R_m = 2\pi n f \lambda^2. \tag{A.8}$$

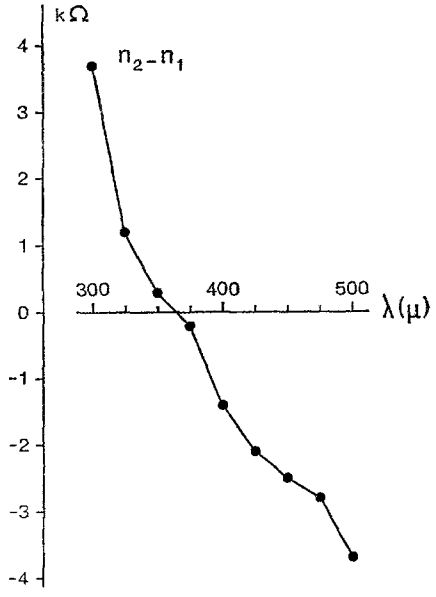

Fig. 9. Relationship between n_2-n_1 and λ; curve intersects the λ-axis at best λ. The best n is then found from Fig. 8 or Eq. (A.5) or (A.6). Note difference in ordinate scale between this figure and Fig. 8

We wish to thank C. C. Hollander-Schoonlingen for valuable technical assistance. We are also indebted to Drs. J. Th. F. Boeles and L. N. Bouman for their interest in this work, to A. A. Meijer and J. R. van Leeuwen who designed and built part of the electronical apparatus, and to A. W. Schreurs who designed and built the micro-manipulators.

This work was aided in part by a grant from the Netherlands Organization for the Advancement of Pure Research (ZWO).

References

Abramowitz, M., Stegun, I. A. 1964. Handbook of Mathematical Functions. National Bureau of Standards, Washington, D.C.

Azarnia, R., Loewenstein, W. R. 1971. Intercellular communication and tissue growth. V. A cancer cell strain that fails to make permeable membrane junctions with normal cells. *J. Membrane Biol.* **6**:368.

Barr, L., Dewey, M. M., Berger, W. 1965. Propagation of action potentials and the structure of the nexus in cardiac muscle. *J. Gen. Physiol.* **48**:797.

Cedergren, B., Harary, I. 1964. In vitro studies on single beating rat heart cells. VII. Ultrastructure of the beating cell layer. *J. Ultrastruct. Res.* **11**:443.

Couch, R. J., West, T. C., Hoff, H. E. 1969. Development of the action potential of the prenatal rat heart. *Circulation Res.* **24**:19.

Eisenberg, R. S., Johnson, E. A. 1970. Three dimensional electrical field problems in physiology. *In:* Progress in Biophysics and Molecular Biology. J. A. V. Butler and D. Noble, editors. Vol. 20, p. 1. Pergamon Press, Oxford.

Frank, K., Fuortes, M. G. F. V. 1956. Stimulation of spinal motoneurons with intracellular microelectrodes. *J. Physiol.* **134**:451.

George, E. P. 1961. Resistance values in a syncytium. *Aust. J. Exp. Biol. Sci.* **39**:267.

Goshima, K. 1970. Formation of nexuses and electrotonic transmission between myocardial and FL cells in monolayer culture. *Exp. Cell Res.* **63**:124.

Harary, I., Farley, B. 1963. In vitro studies on single beating rat heart cells. I. Growth and Organisation. *Exp. Cell Res.* **29**:451.

Heppner, D. B., Plonsey, R. 1970. Simulation of interaction of cardiac cells. *Biophys. J.* **10**:1057.

Hyde, A., Blondel, B., Matter, A., Cheneval, J. P., Filloux, B., Girardier, L. 1969. Homo and heterocellular junctions in cell cultures: An electrophysiological and morphological study. *In:* Progress in Brain Research. K. Akert and P. G. Waser, editors. Vol. 31, p. 283. Elsevier Publishing Co., Amsterdam.

Jongsma, H. J., Hollander, C. C. 1971. Synchronisation of cardiac pacemaker cells. *Pflüg. Arch. Ges. Physiol.* **328**:263.

Kloot, W. G. van der, Dane, B. 1964. Conduction of the action potential in the frog ventricle. *Science* **146**:74.

Lehmkuhl, D., Sperelakis, N. 1963. Transmembrane potentials of trypsin-dispersed chick heart cells cultured in vitro. *Amer. J. Physiol.* **205**:1213.

Lehmkuhl, D., Sperelakis, N. 1965. Electrotonic spread in cultured chick heart cells. *J. Cell. Comp. Physiol.* **66**:119.

Loewenstein, W. R., Kanno, Y. 1964. Studies on an epithelial (gland) cell junction. I. Modifications of surface membrane permeability. *J. Cell Biol.* **22**:565.

Loewenstein, W. R., Socolar, S. J., Higashino, S., Kanno, Y., Davidson, H. 1965. Intercellular communication: Renal, uninary bladder, sensory and salivary gland cells. *Science* **149**:295.

Marcus, P. I., Cieciura, S. J., Puck, T. T. 1956. Clonal growth in vitro of epithelial cells from normal human tissues. *J. Exp. Med.* **104**:615.

Noble, D. 1962. The voltage dependence of the cardiac membrane conductance. *Biophys. J.* **2**:381.

Pager, J., Bernard, C., Gargouil, Y. M. 1965. Evolution au cours de la croissance foetale de effets de l'actylcholine au niveau de l'oreillette de rat. *Compt. Rend. Soc. Biol.* **159**:2470.

Politoff, A. L., Socolar, S. J., Loewenstein, W. R. 1969. Permeability of a cell membrane junction. Dependence on energy metabolism. *J. Gen. Physiol.* **53**:498.

Sakamoto, Y., Goto, M. 1970. A study of the membrane constants in the dog myocardium. *Jap. J. Physiol.* **20**:30.

Schanne, O. 1969. Measurement of cytoplasmatic resistivity by means of the glass microelectrode. *In:* Glass Microelectrodes. M. Lavallee, O. F. Schanne, and N. C. Hebert, editors. p. 299. John Wiley and Sons, Inc., New York.

Shiba, H. 1971. Heavyside's "Bessel cable" for flat simple epithelial cells with low resistive junctional membranes. *J. Theoret. Biol.* **30**:59.

Siegenbeek van Heukelom, J. 1971. Cell communication in epithelial systems. Ph. D. Thesis. University of Utrecht, The Netherlands, and Bronder-Offset, Rotterdam.

Sjöstrand, F. S., Anderson, E. 1954. Electron microscopy of the intercalated disks of cardiac muscle tissue. *Experientia* **10**:369.

Sperelakis, N. 1969. Lack of electrical coupling between contiguous myocardial cells in vertebrate hearts. *In:* Comparative Physiology of the Heart: Current Trends. F. W. McCann, editor. p. 135. Birkhauser, Basel.

Sperelakis, N., Hoshiko, T., Berne, R. M. 1960. Nonsyncytial nature of cardiac muscle: Membrane resistance of single cells. *Amer. J. Physiol.* **198**:531.

Sperelakis, N., Lehmkuhl, D. 1964. Effect of current on transmembrane potentials in cultured chick heart cells. *J. Gen. Physiol.* **47**:895.

Spira, A. W. 1971. The nexus in the intercalated disk of the canine heart: Quantitative data for an estimation of its resistance. *J. Ultrastruct. Res.* **34**:409.

Tanaka, I., Sasaki, Y. 1966. The electrotonic spread in cardiac muscle of the mouse. *J. Gen. Physiol.* **49**:1089.

Tille, J. 1966. Electrotonic interaction between muscle fibers in the rabbit ventricle. *J. Gen. Physiol.* **50**:189.

Trautwein, W., Kuffler, S. W., Edwards, C. 1956. Changes in membrane characteristics of heart muscle during inhibition. *J. Gen. Physiol.* **40**:135.

Weidmann, S. 1952. The electrical constants of Purkinje fibres. *J. Physiol.* **118**:348.

Weidmann, S. 1966. Diffusion of radiopotassium across intercalated disks of mammalian cardiac muscle. *J. Physiol.* **187**:323.

Weidmann, S. 1970. Electrical constants of trabecular muscle from mammalian heart. *J. Physiol.* **210**:1041.

Wollenberger, A. 1964. Rhythmic and arrhythmic contractile activity of single myocardial cells cultured in vitro. *Circulation Res. (Suppl. II)*, *XIV–XV*:184.

Woodbury, J. W. 1962. Cellular electrophysiology of the heart *In:* Handbook of Physiology. W. F. Hamilton, editor. Sect. 2, Circulation I, p. 237, American Physiological Society, Washington, D.C.

Woodbury, J. W., Crill, W. E. 1961. On the problem of impulse conduction in the atrium. *In:* Nervous Inhibition. E. Florey, editor. p. 124. Pergamon Press, Oxford.

Woodbury, J. W., Crill, W. E. 1970. The potential in the gap between two abutting cardiac muscle cells. *Biophys. J.* **10**:1076.